ARTICLE

Contact Electrochemical Replication of Hydrophilic−Hydrophobic Monolayer Patterns

Assaf Zeira,[†] Devasish Chowdhury,[†,‡] Rivka Maoz,* and Jacob Sagiv*

Department of Materials and Interfaces, The Weizmann Institute of Science, Rehovot 76100, Israel. [†]Equally contributing authors. [‡]Present address: Centre for Nanotechnology, Indian Institute of Technology Guwahati, Guwahati-781039, Assam, India.

ABSTRACT Contact electrochemical replication (CER) is a novel pattern replication methodology advanced in this laboratory that offers the unprecedented capability of direct one-step reproduction of monolayer surface patterns consisting of hydrophilic domains surrounded by a hydrophobic monolayer background (hydrophilic @ hydrophobic monolayer patterns), regardless of how the initial "master" pattern was created. CER is based on the direct electrochemical transfer of information, through aqueous electrolyte bridges acting as an information transfer medium, between two organosilane monolayers self-assembled on smooth silicon wafer surfaces. Upon the application of an appropriate voltage bias between a patterned monolayer/silicon specimen playing the role of "stamp" and a monolayer/silicon specimen playing the role of "target", the hydrophilic features of the stamp are copied onto the hydrophobic surface of the target. It is shown that this electrochemical printing process may be implemented under a variety of experimental configurations conducive to the formation of nanometric electrolyte bridges between stamp and target; however, using plain liquid water for this purpose is, in general, not satisfactory because of the high surface tension, volatility, and incompressibility of water. High-fidelity replication of monolayer patterns with variable size of hydrophilic features was achieved by replacing water with a sponge-like hydrogel that is nonvolatile, compressible, and binds specifically to the hydrophilic features of such patterns. Since any copy resulting from the CER process can equally perform as stamp in a subsequent CER step, this methodology offers the rather unique option of multiple parallel reproduction of an initially fabricated master pattern.

KEYWORDS: monolayer patterning · AFM · organosilane monolayers · surface wetting · pattern replication · electrochemistry · hydrogels

*Address correspondence to jacob.sagiv@weizmann.ac.il, rivka.maoz@weizmann.ac.il.

Received for review August 15, 2008 and accepted October 15, 2008.

Published online December 9, 2008. 10.1021/nn8005174 CCC: $40.75

Considerable efforts have been and continue to be devoted in recent years to the advancement of new methods of surface patterning—an issue of obvious central importance for progress in the area of nanofabrication. At present, one is faced with a variety of "unconventional" methods of surface patterning, each of which makes use of a different physical or chemical principle of operation[1] and offers specific advantages for different specific applications. En route to a comprehensive nanofabrication methodology by chemical means (the so-called bottom-up approach), this laboratory has advanced constructive nanolithography (CNL)[2] and constructive microlithography (CML),[3] collectively referred to as constructive lithography (CL), as a generic approach to the nondestructive chemical patterning of highly ordered organosilane monolayers. CL exploits electrochemical transformations that preserve the structural integrity of the patterned monolayer and so allow its direct further utilization as a template in various postpatterning processes of template-guided self-assembly and surface chemical modification.[2−14]

In CNL, an electrically biased scanning force microscope (SFM) tip bearing a nanodroplet of water produced by spontaneous capillary condensation from the ambient is typically used to oxidize terminal $-CH_3$ functions of an OTS/Si monolayer to $-COOH$[2] (OTS/Si denotes a self-assembled monolayer on silicon derived from the *n*-octadecyltrichlorosilane, $SiCl_3—(CH_2)_{17}—CH_3$, molecular precursor[2,8,15]). In this manner, planned patterns of nanometric hydrophilic sites can be inscribed on the highly hydrophobic top surface of an OTS monolayer. In CML, monolayer patterns consisting of hydrophilic surface regions of micrometric and larger dimensions are analogously created onto a hydrophobic OTS surface using a conductive stamp, which allows the entire desired pattern to be simultaneously printed rather than serially inscribed with a scanning probe.[3]

Both CNL and CML combine methods of surface self-assembly, and particularly organic monolayer self-assembly, with electrochemical oxidation/reduction processes mediated by an interfacial aqueous medium confined to the contact area between a conductive SFM tip or a conductive stamp and a conductive monolayer-coated target surface (typically but not only[4,5] OTS/Si) on which the desired pattern is inscribed (tip)[2,4,5,16] or printed (stamp).[3] As such, CL

is related, on the one hand, to surface patterning methods such as microcontact printing (μCP),[1,8,17−21] dip-pen nanolithography (DPN)[22−25] and scanning near-field photolithography (SNP)[26] and, on the other hand, to local oxidation lithography (LOL).[27−30] In a typical configuration, μCP employs a topographically patterned polymeric stamp to locally deliver a molecular "ink" that forms a self-assembled monolayer on the target surface (typically alkanethiols on gold) in the areas contacted by the protruding features of the stamp.[1] DPN employs an SFM tip as tool for planned delivery of molecular "inks" to preselected sites on the target surface (typically alkanethiols on gold, like in the μCP process).[22,24] SNP uses a scanning near-field optical tip to locally modify appropriate monolayers by photochemical transformations,[26] and LOL is an electrochemical method that operates similarly to CL, the pattern being, however, created by the local oxidation of the target surface itself (*e.g.*, silicon).[27]

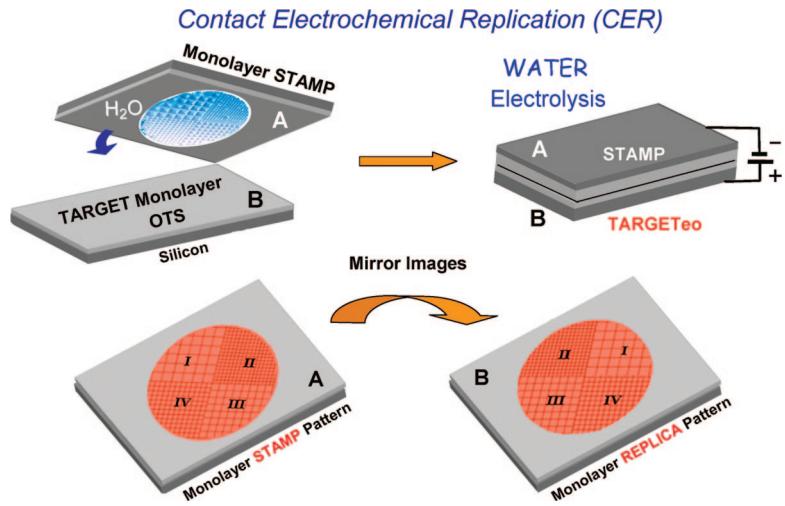

Figure 1. Schematic representation of the CER process: A patterned organosilane monolayer consisting of hydrophilic surface regions (coated with a thin layer of water or of a suitable water absorbing material) surrounded by a hydrophobic, water-free OTS/Si background (monolayer STAMP, A) is pressed against a hydrophobic OTS/Si monolayer (TARGET monolayer, B) (top left). Upon the application of an appropriate voltage bias between A and B, with B positively biased (top right), the hydrophilic features of the STAMP are reproduced onto the TARGETeo (electrooxidized target). The electrochemically printed replica pattern (B), consisting of hydrophilic OTSeo/Si (electrooxidized OTS) features surrounded by a hydrophobic OTS/Si monolayer background (OTSeo@OTS), is a mirror image of the monolayer stamp pattern (A) (bottom).

CL offers a series of rather unique capabilities compared with other methods of surface patterning, which make it particularly well suited as a platform for bottom-up nanofabrication.[2−14] However, regardless of the specific physical or chemical process utilized in the creation of a particular surface pattern, all known methods of surface patterning are equally plagued by the apparent incompatibility of ultimate miniaturization with speed; in general, fast parallel methods like photolithography or printing (including μCP and CML) do not reach the smallest desired dimensions, whereas methods that may in principle go down to the nanoscale, like the various scanning probe nanolithographies (including DPN, SNP, LOL, and CNL) are serial techniques and thus too slow for most practical purposes. Is this an inherent fundamental limitation or might there be ways to overcome it? Using large arrays of tips working in parallel, DPN strives to reach high throughput and cover centimeter-size surfaces while preserving the serial mode of pattern writing at the level of the individual tip.[25] Here we present a series of experimental results that hold promise for the advancement of a true parallel approach to this basic problem, building on the recently demonstrated new concept of contact electrochemical replication (CER) of hydrophilic @ hydrophobic monolayer patterns[31] (Figure 1).

As illustrated in Figure 1, the hydrophilic features of a "monolayer stamp" (A), conveniently produced by the appropriate patterning of a highly hydrophobic OTS/Si monolayer, may be copied electrochemically onto the surface of a pristine OTS/Si "target monolayer"(B) brought in contact with the stamp upon the application of an appropriate voltage bias between stamp and target, provided a thin layer of water or of a suitable water absorbing material is present at the interface between the hydrophilic features of the stamp and the target. In this CER process, the monolayer stamp (A) plays the role of cathode and the target monolayer (B) of anode, in a manner analogous to the electrochemical inscription of nanopatterns with a conductive SFM tip[27,28,2,4,16] (in CNL) or the printing of micropatterns with a conductive metal stamp[3,29,30] (in CML). At the cathode (stamp), regular electrolysis of water conceivably results in liberation of hydrogen[5,27] (with preservation of the stamp pattern), whereas at the anode, the terminal $-CH_3$ groups of the target monolayer (OTS) are electrochemically oxidized to $-COOH$ (OTSeo),[2] the OTS $\rightarrow$ OTSeo conversion (and possibly additional regular liberation of oxygen[5]) being confined to surface regions of the target facing the hydrophilic regions of the stamp:

$$\text{STAMP reaction (cathode): } 2H_2O + 2\,e^- \rightarrow H_2 + 2OH^-$$

$$\text{TARGET reaction (anode): } -CH_3 + 2H_2O \rightarrow -COOH + 2H_2 + 2H^+ + 2e^-$$

$$\text{overall process: } -CH_3\text{(TARGET)} + 2H_2O \rightarrow -COOH\ \text{(TARGETeo)} + 3H_2$$

In principle, this water-mediated process thus offers a straightforward means for the direct replication of information stored on a smooth silicon surface in the form of wetting contrast between the hydrophilic and hydrophobic domains of a patterned organic mono-

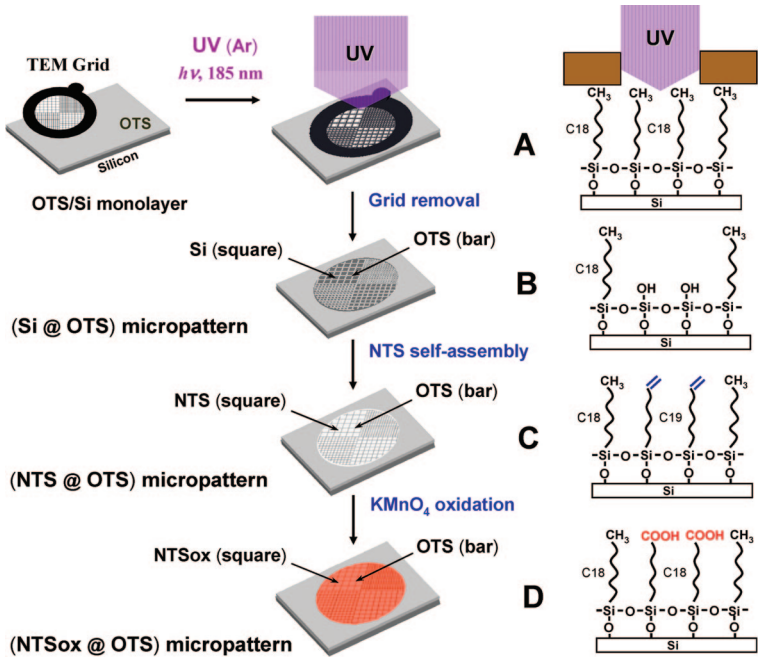

Figure 2. Fabrication of hydrophilic @ hydrophobic monolayer micropatterns for use as CER stamp patterns with well-defined molecular structure and surface functionality: Local removal of the alkyl tails of a self-assembled OTS/Si monolayer, *via* photocleavage in areas selected by UV irradiation through a TEM (transmission electron microscope) grid employed as contact mask (A, B), is followed by self-assembly of NTS in the irradiated areas (C) and final conversion of NTS to NTSox (oxidized NTS) *via* wet chemical oxidation of its terminal vinyl group to −COOH (D). The resulting monolayer pattern (NTSox@OTS) consists of hydrophilic NTSox/Si squares and hydrophobic OTS/Si bars, surrounded by a hydrophobic OTS/Si monolayer background.

herent inability of two rigid surfaces to establish intimate molecular contacts over macroscopic geometrical areas of contact.[3] The resulting electrochemical transformation is thus effectively confined to the interfacial water bridges connecting the two surfaces, dry points of contact remaining inactive. Consequently, to ensure faithful pattern replication, the formation of such water bridges needs to be strictly confined to the hydrophilic features of the stamp.

While the basic feasibility of the CER process has been demonstrated, the preliminary results obtained in the proof-of-concept experiments reported previously[31] were far from satisfactory, apparently because of poor selectivity in the confinement of water bridges to the hydrophilic regions of the stamp pattern. As surface condensation from the ambient was also employed for the optical imaging of both the stamp and replica patterns, insufficient selectivity in the preferential condensation of water on hydrophilic monolayer features further contributed to the apparent low quality of the information transfer in these first CER experiments.[31] Here we show how these difficulties may be overcome so as to achieve high fidelity in the contact electrochemical replication of hydrophilic @ hydrophobic monolayer patterns. This paper is devoted to a comprehensive study of the replication of hydrophilic monolayer features spanning lateral dimensions in the micrometer−centimeter range, which allows an unequivocal chemical-structural characterization, by the combined application of optical imaging, SFM, and quantitative FTIR (Fourier transform infrared) and micro-FTIR spectroscopy, of both the stamp and corresponding replica patterns. Issues of spatial resolution as well as the possible extension of the CER approach down to the nanoscale are outside the scope of this work and will be addressed in future publications.

layer assembled on it, regardless of how the initial hydrophilic @ hydrophobic monolayer pattern was created. Here, water plays the essential triple role of electrochemical reagent, electrolyte, and conformal information transfer medium facilitating uniform transfer of information between the contacting surfaces involved in the electrochemical process, despite the in-

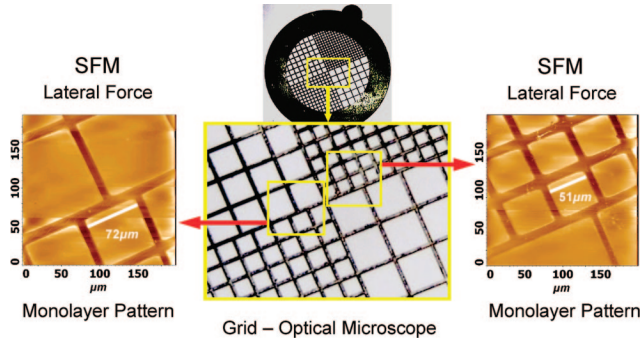

Figure 3. Example of a variable TEM grid with four different quadrants (SPI, GVHS Fine Square Mesh, Nickel) used as contact mask in the pattern fabrication process (steps A and B in Figure 2), and SFM images of two regions of the final NTSox@OTS monolayer micropattern (step D in Figure 2) corresponding to the two yellow frames in the optical image of the central region of the TEM grid. The metal bars of the grid have constant width while the widths of the square holes vary from one quadrant to the other. As expected, the contrast in the lateral force SFM images is indicative of higher friction within the hydrophilic NTSox squares compared to the hydrophobic OTS bars.[2,3,16]

RESULTS AND DISCUSSION

Fabrication of Monolayer Stamp Patterns. Monolayer stamp micropatterns exposing well-defined hydrophilic and hydrophobic features, in terms of their molecular structure and surface-exposed functionality (−COOH and respectively $-CH_3$), were fabricated as depicted in Figure 2, by mask-defined local photocleavage of the alkyl tails of a self-assembled OTS/Si monolayer,[6,32,33] followed by back filling of the empty spaces thus created with a self-assembled NTS/Si monolayer (NTS/Si denotes a monolayer derived from the nonadecenyltrichlorosilane, $SiCl_3—(CH_2)_{17}—CH═CH_2$, molecular precursor[2,4,7,15]), and final conversion of NTS to NTSox (oxidized NTS) *via in situ* chemical oxidation of its terminal vinyl function to −COOH.[4] As shown in Figure 3, this pattern fabrication route can

yield good monolayer patterns with rather sharp boundaries (on a micrometer scale) between OTS (hydrophobic) and NTSox (hydrophilic) surface regions, as defined by the metal bars and, respectively, square holes of the contact mask used in the photocleavage patterning step (Figure 2, A and B).

WATER — Its Key Role and Limitations. Monolayer stamp patterns fabricated by the procedure depicted in Figure 2 have been tested in a series of exploratory CER experiments conducted with the purpose of identifying experimental conditions under which high-fidelity replicas may be obtained. Using a purpose-designed cell that allows fine control of both the environmental relative humidity (RH) and surface temperature (within ~5% RH and ± 0.1 °C; see Experimental Section), it became possible to generate water condensation patterns of dramatically improved quality (compared to those previously reported)[31] *via* preferential condensation on the hydrophilic features of hydrophilic @ hydrophobic monolayer patterns of the kind employed as stamps or obtained as replicas in the CER process (Figure 4). However, while such water/monolayer condensation patterns serve well the purpose of optical imaging of the respective underlying monolayer patterns (which by themselves are not optically visible), their performance as CER stamps is, in general, limited. Like any liquid, plain liquid water is incompressible and so may perform well as information transfer medium in the CER process only as long as a water film of uniform thickness forms on all hydrophilic features of the monolayer stamp pattern, regardless of their lateral dimensions and shapes. In general, this is a rather improbable situation. Water is volatile and its high surface tension favors the formation of quasi-spherical (droplet-like) features,[34] as also indicated by the appearance of the crossing points of the water bars in the bottom image in Figure 4. Thus, it is practically impossible to generate stable water patterns of uniform thickness on top of hydrophilic monolayer features with variable lateral dimensions and aspect ratios. Moreover, one cannot easily follow and so control the formation of water patterns with dimensions below those accessible by optical microscopy, while the characterization of liquid features by SFM techniques is difficult and rather impractical for our purpose.[10] Although in general unlikely to yield satisfactory results, plain liquid water was successfully employed as information transfer medium in a CER experiment carried out with the purpose of providing direct spectral evidence on the nature of the monolayer transformation induced by a uniform macro-size NTSox/Si monolayer stamp in a target OTS/Si specimen of comparable dimensions (*ca.* 3.5 cm × 2 cm), which is well suited for acquisition of quantitative infrared spectra in the Brewster angle configuration[35,15](Figure 5).

The main spectral features of interest in Figure 5 are the 2964 cm^{-1} and 2879 cm^{-1} methyl bands of OTS[15,35] (curve a), which are missing in both NTSox and

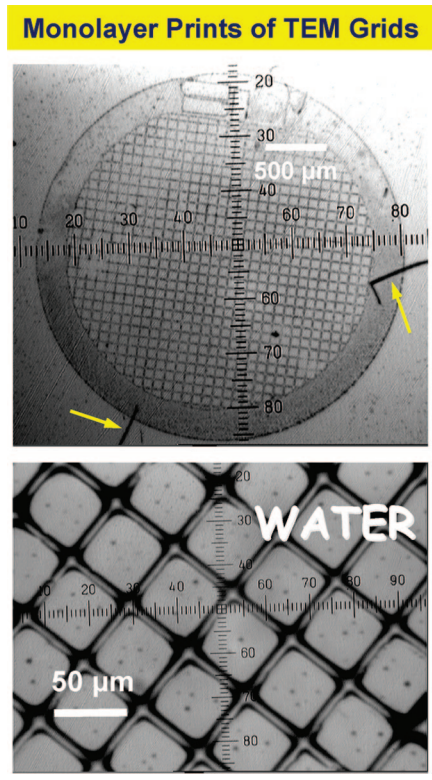

Figure 4. Examples of optical micrographs of water condensation patterns generated by preferential condensation under precise humidity and temperature control (in a specially built humidity cell) on the hydrophilic OTSeo regions of OTSeo@OTS monolayer patterns produced electrochemically on OTS/Si monolayers with TEM copper grid stamps (CML process).[3] The electrochemical printing was done with a voltage bias of 10 V (stamp negative, target ground) applied for 10 s while manually pressing the TEM grid stamp against the OTS/Si target (with the help of an eraser-caped pencil), immediately after brief exposure of the grid to saturated water vapor above a beaker filled with hot water. Currents of the order of 5 mA were measured during the printing of the patterns. Since such monolayer patterns are not optically visible in the absence of surface condensed water, scratch markers help locate them on the surface of the target (indicated by the two yellow arrows).

OTSeo spectra (curves b and c), the identical peak positions and band widths, and almost identical peak absorbance of the 2917, 2850, and 1467 cm^{-1} methylene bands[15,35] in all three curves, and the similar −COOH bands around 1718 cm^{-1} in the NTSox[15,35] and OTSeo curves. These observations unequivocally demonstrate that the electrochemical transformation converting OTS/Si to OTSeo/Si is limited to the top $-CH_3$ groups of OTS only, which are quantitatively oxidized to −COOH with full preservation of the molecular organization of the inner core of the monolayer. Thus, the alkyl tails in OTSeo/Si retain the extended all-trans conformation, perpendicular orientation, and dense, solidlike packing characteristic of its OTS/Si precursor and similar highly ordered organosilane monolayers.[15] The small decrease in the peak absorbance of the $-CH_2-$ stretch bands around 2900 cm^{-1} upon the conversion of OTS to OTSeo may be indicative of some damage caused to the reacted monolayer in this particular

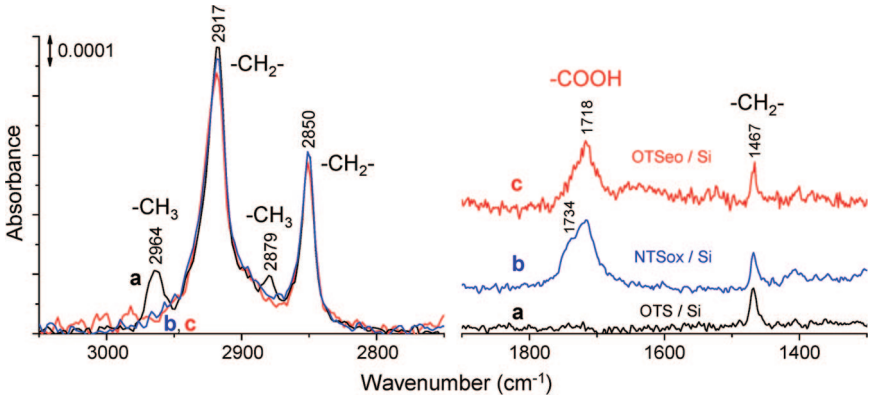

Figure 5. Quantitative Brewster angle FTIR spectra[35,15] of macrosize OTS/Si target (a, black curve), NTSox/Si stamp (b, blue curve), and OTSeo/Si replica (c, red curve) produced upon the application, for 1 min, of a bias voltage of 40 V between stamp (negative) and target (grounded), the entire CER operation being carried out in a humidity-temperature controlled atmosphere at ~100% RH, 22 °C, using a weight of 1.3 Kg to press the stamp against the target. Currents varying between ~670 μA (initial) to ~400 μA (final) were measured during the application of the voltage bias, with a geometrical area of contact between stamp and target of ~7 cm^2 (see text). The curves represent net spectral contributions of the organic monolayers, after mathematical subtraction of the spectral contributions of the respective bare Si substrates. Since both the stamp and target monolayers were assembled on double-side-polished wafer substrates (see Experimental Section) while the OTSeo/Si replica is the result of an electrochemical transformation that affects only the printed side of the OTS/Si target, to facilitate a direct comparison, all spectral curves were normalized to the corresponding one-side contributions. In the spectral range 1900−1300 cm^{-1}, the blue and red curves are shifted vertically for clarity.

sample,[36] possibly at points of closer contact and higher local electrical fields and current densities than the average (vide infra), which does not, however, affect its overall molecular organization. Finally, by comparison with NTSox (curve b), one may note the missing shoulder at ~1734 cm^{-1} in the C═O stretch band of OTSeo (curve c), assigned to monomeric −COOH species.[15,35,37] It thus appears that the organization of the top −COOH groups of OTSeo is not identical to that of NTSox, the former possibly exhibiting more extensive lateral hydrogen bonding between adjacent acid groups.[35,37]

One may note that although the applied voltage bias in this CER experiment (40 V) was significantly higher than that normally used in the CNL patterning with conductive SFM tips (3−17 V),[2,7,16,14] in the average, the measured current density is here between 2 and 3 orders of magnitude lower. In both cases, the structural stability of the monolayer upon the application of the voltage bias suggests that the effective voltage drop across the monolayer itself may not exceed 3−4 V—the expected threshold of dielectric breakdown in such films.[38] With a printed monolayer area of ~7 cm^2, the maximal measured current density of ~96 μA/cm^2 (670 μA/7 cm^2, assuming uniform current over the entire geometrical area of contact between stamp and target) translates into ~0.192 fA/200 nm^2, which is the equivalent current passing through a surface area comparable to that usually covered by a conductive SFM tip in contact with the monolayer surface in the CNL process.[14] Typical onset writing currents in CNL were found to be of the order of 100 fA, that is, current densities *ca.* 520 times higher than that measured in this CER experiment. A current density of ~0.192 fA/200 nm^2 further translates into ~1.92 × 10^{-4} fA/OTS molecule, or ~1.2 electrons/s/OTS molecule (with 0.2 nm^2 as the molecular area of OTS in a compact, highly ordered monolayer[15,35]). This corresponds to a total charge of ~72 electrons passing in the average through a single OTS molecule during the 1 min printing time. For comparison, in dots inscribed with 3.0 ms voltage pulses applied to a scanning tip,[7] the total charge passing through a single OTS monolayer at a current density of ~100 fA/200 nm^2 (*i.e.*, ~1.0 × 10^{-1} fA/OTS molecule)[39] is ~1.9 electrons, which is the actual limiting charge (2 electrons) required for the electrochemical oxidation (with a 100% yield) of a single $-CH_3$ group to −COOH (*vide supra*).

This analysis suggests that the printing time under experimental conditions like those indicated in Figure 5 might be reduced from a minute to less than 2 s. However, regardless of whether the printing time is 2 or 60 s, the advantage of parallel (one-step) printing of an entire pattern as compared to its serial inscription with a scanning tip should be evident if one realizes that to fill an area of 7 cm^2 (*i.e.*, 7 × 10^{14} nm^2) with a scanning tip inscribing individual dots at the speed of 200 nm^2/3.0 ms would require 1.05 × 10^{10} seconds, the unrealistic time of 332 years!

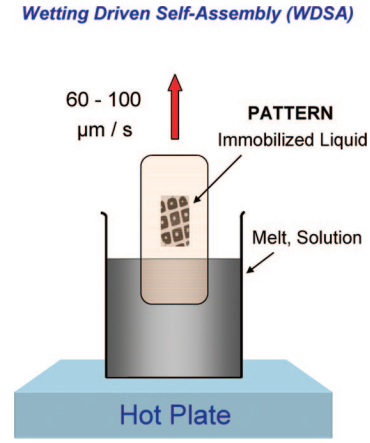

Figure 6. Wetting driven self-assembly (WDSA): Selective retention of a nonvolatile liquid (neat, solution, melt) with appropriate surface tension on the wettable (lyophilic) portion of a monolayer pattern consisting of wettable regions surrounded by a nonwettable (lyophobic) background is achieved upon slow retraction of the monolayer-coated substrate from the liquid.[14] The speed of retraction is conveniently regulated with the help of a motor-driven lift.

Quasi-Water Patterns. To overcome the fundamental obstacles encountered in the utilization of plain liquid water as information transfer medium in the CER process, we undertook a research strategy based on the hypothesis that water might be replaced by water absorbing materials (WAMs) that can simulate water as far as the formation of effective electrolyte bridges in the CER process is concerned, while differing from plain liquid water in a number of other desirable properties. Useful WAMs are thus expected to have low volatility, adhere selectively to the hydrophilic regions of hydrophilic @ hydrophobic monolayer patterns forming WAM/monolayer patterns of variable dimensions and aspect ratios, and be compressible and easily removable from the surface (to allow repeated utilization of the underlying monolayer pattern).

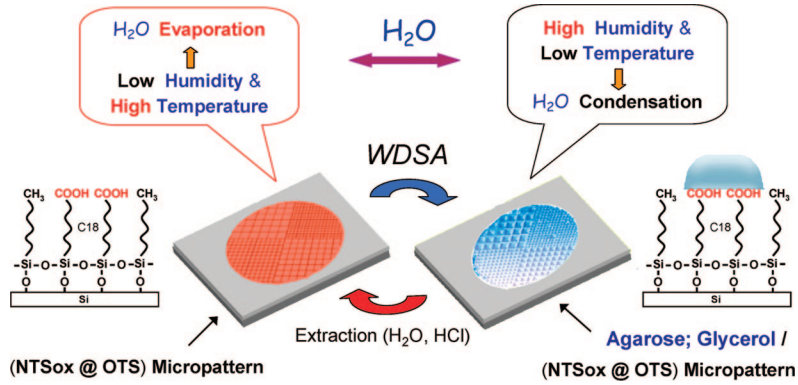

Figure 7. Like water, agarose or glycerol can be selectively and reversibly immobilized on the hydrophilic regions of NTSox@OTS monolayer patterns. Because of rapid evaporation, the formation (by surface condensation) and conservation of such water/monolayer patterns demand precise humidity and temperature control. Unlike water, glycerol/monolayer and agarose/monolayer micropatterns are stable, and so can be easily fabricated by WDSA (Figure 6) and erased by dissolution in water and aqueous HCl. The "agarose; glycerol/(NTSox@OTS) Micropattern" used to illustrate the WDSA process is the actual micrograph of an agarose/monolayer micropattern produced in this manner.

Here we present proof-of-concept experimental results obtained with two very different WAMs, selected with the purpose of identifying similarities as well as expected differences in their modes of action: glycerol, a low molecular weight hygroscopic liquid, and agarose, a high molecular weight polysaccharide polymer forming thermoreversible hydrogels.[42] Both glycerol and dilute aqueous solutions of agarose do not wet methyl-rich hydrophobic surfaces such as that of a highly ordered OTS monolayer but adhere well to the top −COOH groups of NTSox or NTSeo, thus facilitating their selective immobilization on the hydrophilic regions of NTSox@OTS stamp patterns or NTSeo@OTS replica patterns. This is easily achieved by wetting driven self-assembly (WDSA),[14] using the simple experimental setup depicted in Figure 6.

Glycerol was assembled from the neat liquid at the ambient temperature (22 ± 0.5 °C), and agarose from a dilute water solution at 90 °C (see Experimental Section). Upon cooling down and equilibrating with the ambient humidity (RH 50 ± 5%), agarose forms stable hydrogel/monolayer patterns. Due to its low volatility (bp 290 °C), glycerol forms stable liquid/monolayer patterns as well. Thus, unlike water, both glycerol/monolayer and agarose/monolayer stamp patterns are stable and easily handled in ambient conditions without the need of providing precise humidity and temperature control (Figure 7). Glycerol is easily removed from the monolayer pattern by dissolution in water, and agarose by dissolution in hot water and aqueous HCl (see Experimental Section). As discussed in the following, the essential difference between glycerol and agarose is that glycerol, like water, is an incompressible liquid, while agarose hydrogel is a hydrated polymeric network that resembles a flexible water-absorbing sponge which may reversibly swell and contract to a certain extent without loosing its water content.

WAMs Performing Better than Water. Exploratory CER experiments have been carried out with the main purpose of verifying our basic hypothesis regarding the possible utilization of WAMs as effective information transfer media in the CER process. At this stage, no attempt was made to standardize or optimize the experimental protocol, many details of which being varied rather drastically from one experiment to another (*vide infra*) in order to gather data that would allow us improve our understanding of the CER mechanism toward its future optimization. The main results of two successful CER experiments, representative of glycerol and agarose, are discussed in the following.

Glycerol. Exploiting the stability of glycerol/monolayer patterns, glycerol was successfully applied both as an information transfer medium in the CER process and as a visualization developer in the optical imaging of the resulting replica patterns. High quality replicas, virtually identical to the corresponding stamp patterns, were obtained (Figure 8), which attests to the high fidelity of the glycerol-mediated replication process. The presence of water in glycerol is clearly revealed (in the infrared spectra) by the characteristic water bending mode[43] at 1654 cm^{-1}, as well as by the much stronger band around 3344 cm^{-1}, which contains contributions from both water[43] and the alcohol O−H groups of the glycerol[44,45] itself. One may note that although the FTIR microscope was purged with dry nitrogen, no decrease in the intensities of the water bands was observed during the collection of these IR spectra, which points to the high affinity of glycerol for water and, consequently, to its effectiveness as a water-immobilizing agent under regular ambient conditions.

Besides its value as a rather unique tool for the direct monitoring of the water content of surface-immobilized thin films, quantitative FTIR microscopy was found particularly useful in the nondestructive

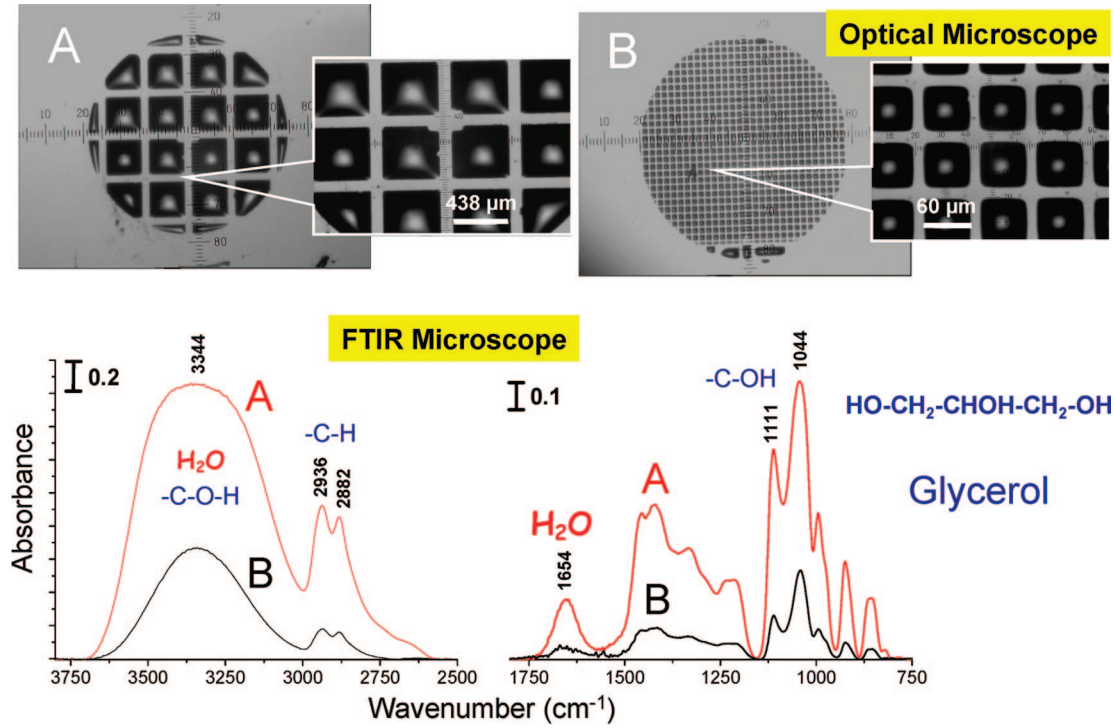

Figure 8. (Top) Optical micrographs of glycerol/(OTSeo@OTS) monolayer replica patterns fabricated by the CER process (Figure 1) with stamps consisting of glycerol/(NTSox@OTS) monolayer micropatterns (Figure 7). Replica A was generated with a voltage bias of 20 V applied for 1 min (measured current ~250 μA) and replica B with 40 V applied for 30 s (measured current 250−300 μA), both under ambient conditions (~50% RH, 22 °C), with the stamp negative and the target grounded. No external pressure was applied between stamp and target. The stamp (not shown) and respective replica patterns (A and B) are practically indistinguishable. (Bottom) Representative micro-FTIR spectra collected from a single square of pattern A and a single square of pattern B (see Experimental Section).

evaluation of the relative thickness of such liquid films. According to the ratios of the −C−H peaks (at 2936 and 2882 cm^{-1}) and the water peaks (at 1654 cm^{-1}) in the glycerol IR spectra (Figure 8), the liquid squares in pattern A are 4.6−4.9 times thicker than those in pattern B. As it has been found in WDSA experiments with both glycerol[46] and other liquids (unpublished results), the thickness of liquid features immobilized by this process on a patterned surface scales up in a rather complex manner with the lateral dimensions of the wettable surface features to which the liquid adheres, implying that monolayer patterns with variable size of wettable features retain liquid films of variable thickness, depending (among a number of additional parameters) on the relative lateral dimensions of the respective pattern features.[46] This limits the usefulness of liquid WAMs such as glycerol to the case of monolayer patterns with wettable features of uniform size, like patterns A and B in Figure 8. The replication of monolayer patterns with wettable regions differing significantly in their lateral size was found to suffer from either or both the coalescence of adjacent liquid features and the mismatch of their different heights in the stamping process. Because of liquid incompressibility, applying external pressure to the stamp in an attempt to establish stamp-target contact in pattern regions with low liquid thickness necessarily results in spillover of the taller liquid features, thus compromising the entire replication process.

Agarose Hydrogel. Experimental data pertaining to some relevant aspects of the structure and composition of a representative agarose/(NTSox@OTS) monolayer micropattern with variable size of wettable features are summarized in Figure 9. Like in the case of glycerol (Figure 8), the thickness of the agarose features is seen to scale up with their lateral dimensions. One may note that the thickness ratio **A**/**B** measured by SFM (200 nm/60 nm = 3.33) compares well with the ratios of each of the absorbance peaks in the IR spectra of squares A (red curve) and B (black curve): 3.5 (3418), 3.1 (2918), 3.3 (1647), 3.3 (1072 cm^{-1}). As the bands at 1072 and 2918 cm^{-1} represent −C−OH and −C−H agarose vibration modes, respectively,[44,45] the 1647 cm^{-1} band is the characteristic bending mode of water,[43] and the 3418 cm^{-1} band contains contributions from the O−H stretching vibrations of both water[43] and agarose,[44,45] these findings point to a very similar distribution, structure, and concentration of water in all these microgel features, regardless of their overall dimensions.

With a molar absorption coefficient of 21.8 ± 0.3 M^{-1} cm^{-1} (determined for the bending mode of bulk water at 1643 cm^{-1}),[43] the measured peak absorbance at 1647 cm^{-1} corresponds to a water layer thickness of 41.4 ± 0.6 nm in square A and 12.4 ± 0.2 nm in square B. This accounts for 20−21% of the total SFM-measured

thickness of each of these microgel features. Since both the SFM and IR data in Figure 9 were obtained at ~55% RH, this figure applies to the agarose microgel in equilibrium with an atmosphere maintained at a relative humidity around 55%. Variations in the ambient humidity were found to affect the water content of the agarose microgel features accordingly. For example, at ~10% RH, the water content of same agarose squares was found to drop to 7−10% of their total SFM-measured thickness, which shrinks to 83−85% of that at ~55% RH (see Supporting Information, Figures S1 and S2).[47]

Experimental results summarized in Figures 10−12 demonstrate the successful high-fidelity replication of a monolayer micropattern with variable size of wettable features (like that of Figure 9) using agarose hydrogel as information transfer medium in the CER process. The faithful replication of the monolayer stamp pattern is confirmed by comparing the lateral dimensions of the different squares of the monolayer stamp pattern (Figures 3 and 10) with the corresponding squares of the monolayer replica pattern (Figure 11) and those of the bilayer @ monolayer pattern generated by the selective self-assembly of an organized top monolayer on the hydrophilic squares of the replica (Figure 12).

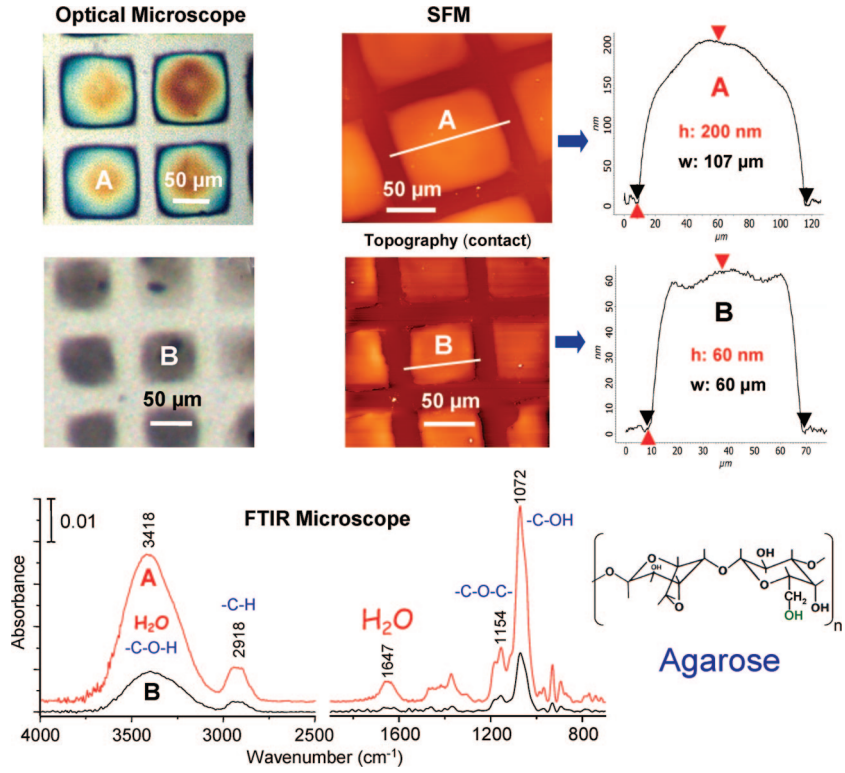

Figure 9. Combined application of optical microscopy, SFM, and quantitative micro-FTIR spectroscopy in the characterization of a typical agarose/(NTSox@OTS) monolayer micropattern with variable size of wettable features. Optical microscopy was used to select two agarose squares, A and B, which were then imaged by SFM and their IR spectra recorded with an FTIR Microscope. Squares A and B are seen to differ considerably in their heights (as indicated by both the interference colors in the respective optical images and the corresponding SFM topographic images and IR absorbance intensities), which scale up with their lateral dimensions. There is good agreement between the heights ratio A/B measured by SFM and the ratios of the absorbance peaks in the IR spectra of squares A and B (recorded with 60 μm × 60 μm and 40 μm × 40 μm microscope apertures, respectively). The IR spectra further allow a quantitative estimation of the water content of the agarose features (see text).

One may note in Figure 10 (images 2 and 3) the contraction/swelling of the agarose features under exposure to variable ambient humidity (also see Supporting Information, Figures S1 and S2) as well as the fact that replication could be achieved only with the hydrogel stamp at 100% RH. It thus appears that only the fully swollen agarose gel can function as an effective electrolyte bridge in the CER process; however, even under such conditions the gel is sufficiently compressible to allow faithful replication of surface features of significantly different dimensions. This remarkable performance suggests that the agarose stamp features can indeed sustain considerable vertical deformation without significant lateral expansion, which points to a sponge-like structure reminiscent of that of certain anisotropic polymer brushes.[48]

The transfer of the pattern from the stamp to the target surface following the application of the voltage bias is immediately apparent owing to the expected redistribution of the agarose hydrogel between the hydrophilic features of the stamp and replica patterns. This is clearly visible in optical micrographs taken immediately after the separation of the two contacting surfaces (not shown). To obtain the water condensation image and the SFM images of the bare replica (image 4 in Figure 10 and Figure 11) as well as reuse the monolayer stamp pattern, the hydrogel coating had to be removed by soaking in boiling water and aqueous HCl (see Experimental Section). Following such treatment, the monolayer stamp pattern employed in this particular experiment could be successfully reused in many CER experiments, carried out over a period of time of several months. No structural deterioration of the NTSox monolayer within the hydrophilic squares of the stamp could be detected by comparing micro-FTIR spectra recorded (as in Figure 11) before and after its multiple reuse. A systematic investigation of the stability of repeatedly reused monolayer stamp patterns as well as of the reproducibility of multiple replication of a given monolayer pattern remains, however, to be performed.

As expected on the basis of previous CNL and CML results,[2,3,7,10,16] the lateral force (friction) within the hydrophilic OTSeo squares of the replica is higher than that measured within the hydrophobic OTS bars while the corresponding topographic contrast is negative, with the OTSeo squares appearing *ca.* 1.6 nm below

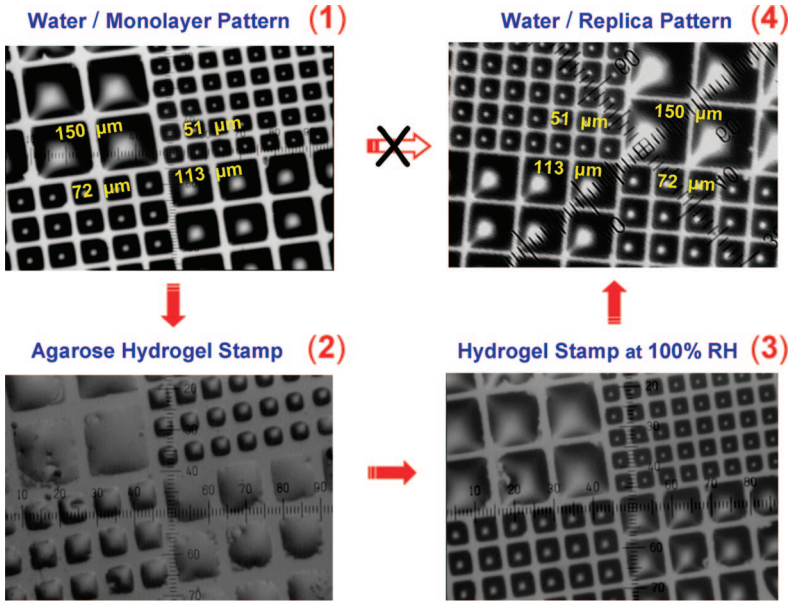

Figure 10. Optical micrographs demonstrating the high-fidelity replication of a NTSox@OTS monolayer micropattern with variable size of wettable features (the same monolayer pattern as in Figure 3) using agarose hydrogel as information transfer medium in the CER process: (1) water condensation image (as in Figure 4) of the NTSox@OTS monolayer micropattern; (2) agarose/(NTSox@OTS) micropattern (agarose hydrogel stamp) under normal ambient conditions (~50% RH, 22 °C); (3) same as panel 2 after equilibration with a saturated water atmosphere (100% RH, 19 °C) in the special humidity cell (hydrogel stamp at 100% RH); (4) water condensation image of the OTSeo@OTS replica pattern produced with the hydrogel stamp at 100% RH (with a voltage bias of 40 V applied for 30 s, the stamp being negative and the target grounded, measured current of 250−300 μA, no external pressure between stamp and target). The replica 4 generated along path 1 → 2 → 3 → 4 is a high-fidelity mirror image of the initial monolayer pattern of panel 1. Direct 1 → 4 pattern transfer, in the absence of agarose, does not yield comparable high quality replicas.

the OTS bars (Figure 11). The observed negative topographic contrast of OTSeo *versus* OTS was shown to represent an artifactal effect of the SFM imaging[3,7,16] rather than the result of eventual structural damaging of the monolayer within the printed regions. This is unequivocally confirmed here by both the quantitative IR spectra in Figures 11 and 12 and the SFM images in Figure 12. As discussed before (Figure 5), the virtually identical methylene bands of OTSeo and OTS, with peak positions at 2916 and 2849 cm^{-1} (Figure 11), indicate that OTSeo, like OTS, is a compact, highly ordered monolayer with all-trans conformation and perpendicular orientation of its hydrocarbon tails. The conversion, within the OTSeo squares, of the top $-CH_3$ groups of OTS to $-COOH$ is evident from the diminished methyl peak absorbance at 2954 cm^{-1}, the residual observed intensity being contributed by the methyls of the OTS monolayer on the back side of this silicon wafer substrate.

That the conversion of $-CH_3$ to $-COOH$ within the OTSeo squares is practically quantitative while the tail methylenes remain intact can be directly deduced from an inspection of the infrared spectra in Figure 12, where the complete disappearance of the methyl peak at 2956 cm^{-1} is clearly identified on the methyl-free background contributed by the NTS monolayer present here on the back side of the silicon substrate. Finally, the assembly of a top NTS monolayer on OTSeo is seen to result in a proportional growth of the methylene bands, their invariant widths and peak positions at 2916 and 2849 cm^{-1} bearing evidence for the formation of a complete, highly ordered top monolayer, structurally indistinguishable from the bottom OTSeo or OTS monolayers. This conclusion is corroborated by the measured topographic difference of ~2.7 nm between the bilayer and monolayer pattern features (Figure 12), as expected for a compact and well-ordered NTSox monolayer covering the OTSeo regions.[7,15] Thus, unlike the apparent depth of the hydrophilic OTSeo squares in the OTSeo@OTS monolayer pattern (Figure 11), the hydrophilic NTSox/OTSeo bilayer squares in the NTSox/OTSeo@OTS pattern (Figure 12) display normal positive topographic contrast along with the expected higher friction relative to the hydrophobic OTS bars. While the reason for the different behavior of the hydrophilic bilayer and monolayer features remains to be clarified, the consistency of the SFM and IR data in Figure 12 would not be possible unless the negative topographic contrast of OTSeo *versus* OTS in the OTSeo@OTS replica pattern (Figure 11) were not an imaging artifact. Furthermore, the self-assembly of a homogeneous and highly ordered top monolayer on the squares of the replica pattern implies that the squares must be covered by a homogeneous and highly ordered OTSeo bottom monolayer template,[7] produced by the (nondestructive) quantitative conversion of the terminal $-CH_3$ groups of OTS to $-COOH$.

Some Control Experiments. A bias voltage of 40 V was applied for 1min to a pair of OTS/Si specimens (1 cm × 1 cm each) pressed together with a total external force of ~15 Kg, first in the ambient atmosphere (55% RH, 21−22 °C) and then in an high humidity atmosphere (96% RH, 21−22 °C). The measured currents, ~700 μA at 55% RH and ~1540 μA at 96% RH, are significantly higher than those recorded in the CER experiments discussed before (Figures 5, 8, and 10). Contact angle measurements complemented by quantitative infrared spectra and SFM images recorded before and after the application of the voltage bias unequivocally demonstrate that, regardless of ambient humidity, the OTS monolayers suffered no transformation or damage upon the application of the voltage bias. These results show that (i) significant electrical currents may pass through two contacting monolayer/Si specimens to which a voltage bias is applied also in the absence of interfacial electrolyte bridges that promote electrochemical monolayer transformations; (ii) large variations in the magnitude of the measured current can be expected depending on experimental variables such as

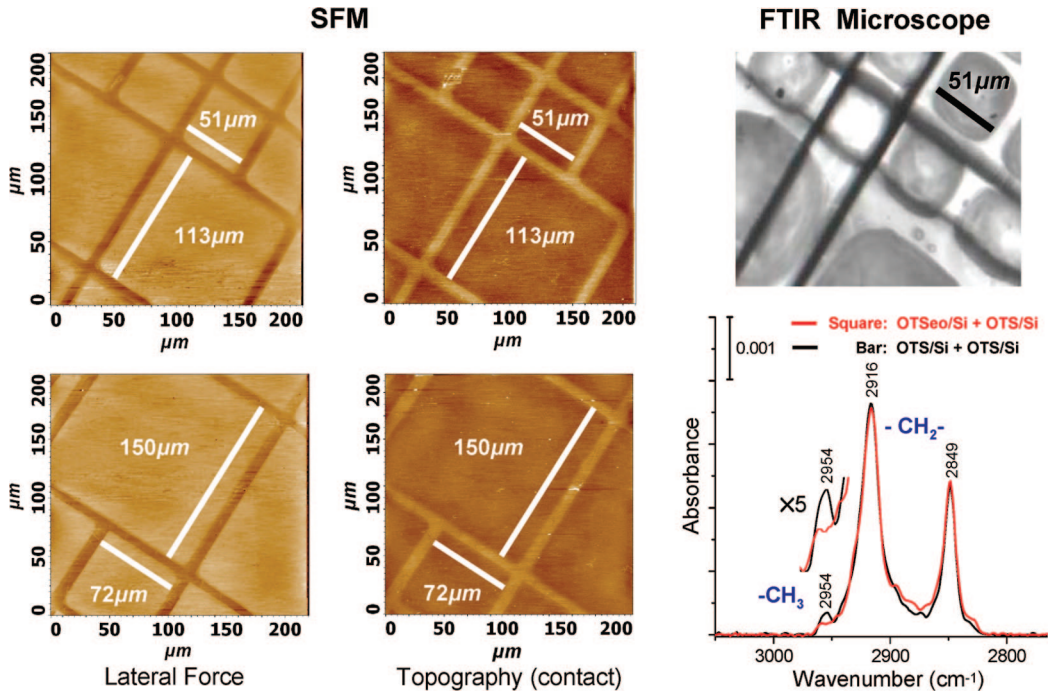

Figure 11. SFM images showing the four different OTSeo squares of same OTSeo@OTS replica pattern as in Figure 10, and micro-FTIR spectra recorded (with a 75 μm × 75 μm microscope aperture) from one of the 150 μm × 150 μm OTSeo squares and from an equivalent unmodified OTS region of same specimen, which is representative of the OTS bars (bottom right). The notation OTSeo/Si + OTS/Si and OTS/Si + OTS/Si is used to indicate the fact that, being measured in transmission through the silicon wafer substrate, these IR spectra contain also the contribution of the back side of the wafer which is coated with a regular OTS monolayer. To enable visualization of the replica pattern and focusing of the IR beam on the desired surface site, the aperture of the FTIR microscope was superimposed on a water condensation image of the replica (*e.g.*, top right), the IR data being then collected after complete evaporation of the water.

applied voltage, applied mechanical pressure (effective area of contact), environmental humidity, and the nature and resistance of the contacts to the silicon specimens. It follows that establishing a correlation between the current measured in a particular CER experiment and the size and/or quality of the resulting monolayer replica pattern may not possible in the absence of effective control of each of these experimental parameters and a proper understanding of their interplay. These aspects of the CER process remain to be clarified in future work.

CONCLUDING REMARKS

Taken together, the experimental results presented here establish contact electrochemical replication (CER) as a viable methodology for the direct electrochemical generation of copies of monolayer surface patterns consisting of hydrophilic domains surrounded by a hydrophobic monolayer background. The effective discrimination between wettable and nonwettable features of a monolayer pattern plays a central role in the CER process. Therefore, the use of highly ordered, defect-free OTS monolayers (exposing low-energy outer surfaces that are not wetted by a large variety of both aqueous and organic liquids — see Experimental Section) is a necessary precondition for its successful implementation.

As in the electrochemical printing with metal or other types of conductive stamps (*e.g.*, Figure 4),[3,13,29,30] the voltage-current relationship in the CER process and the related issue of the effective potential drop across the organic monolayers (target and stamp) are important open questions that remain to be addressed in future research. The different experimental conditions tested in the course of this work and found to yield good replica patterns (Figures 4, 5, 8, and 10) provide a promising starting point, further work being needed *en route* to a comprehensive rationalization of the CER process and its optimization.

While the full range of applicability of this methodology remains to be established, there appears to be virtually no upper limit to the size of hydrophilic features that can be copied by the CER process. Thus, CER offers a simple novel route to the functionalization of macroscopic surface areas *via* the straightforward conversion of exposed $-CH_3$ groups of *n*-alkylsilane monolayers to $-COOH$ (Figure 5). As far as small pattern features are concerned, high-fidelity replication down to micrometer-sized features has been demonstrated here by replacing plain liquid water with a compressible hydrogel coating that acts as an effective quasi-water information transfer medium in the CER process (Figure 10). The agarose hydrogel selected for this study is a representative example of a water absorbing ma-

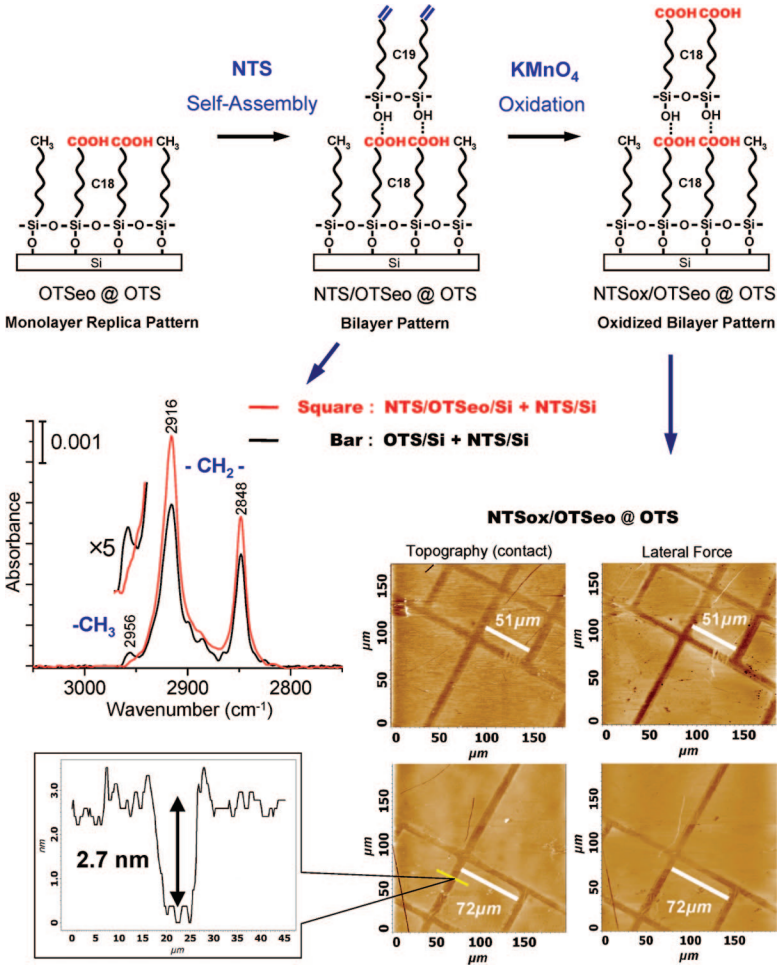

Figure 12. Selective self-assembly of NTS on the OTSeo squares of the OTSeo@OTS replica pattern shown in Figure 11 results in a hydrophobic bilayer @ hydrophobic monolayer pattern (NTS/OTSeo@OTS) which is further converted, by *in situ* oxidation of the terminal vinyl groups of NTS to −COOH (NTSox), into a hydrophilic bilayer @ hydrophobic monolayer pattern (NTSox/OTSeo@OTS). The SFM images of the NTSox/OTSeo@OTS pattern (bottom right) and the measured height difference between the bilayer squares and the monolayer bars separating them (bottom left), together with the micro-FTIR spectra recorded (as in Figure 11) from one of the large NTS/OTSeo squares and an equivalent unmodified OTS region of same specimen (middle left), confirm the successful formation of a homogeneous, highly ordered bilayer within the squares of the replica pattern (see text). As the IR spectra were measured in transmission through the silicon substrate and so contain also the contribution of the back side of the silicon wafer, to emphasize the quantitative disappearance of the terminal $-CH_3$ groups of OTS within the squares of the replica pattern, the initial OTS back-side coating of the Si substrate was removed by photocleavage (as in Figure 2) and replaced with NTS, which protects the sample from adventitious contamination while being devoid of a terminal methyl (see Experimental Section). The notation NTS/OTSeo/Si + NTS/Si and OTS/Si + NTS/Si is thus used to indicate the contribution of the back side NTS monolayer to both the square (NTS/OTSeo/Si) and bar (OTS/Si) spectra.

terial with the desired sponge-like properties; it is not necessarily the optimal choice of such materials. Given the large variety of organic and inorganic hydrogels available, the present promising results obtained with agarose pave the way to a systematic investigation of the utilization of hydrogels for this purpose.

If further developed and optimized, the CER methodology is expected to offer a series of exclusive capabilities compared with other methods of surface patterning and bottom-up assembly:

- CER is rather unique in that it is a printing process enabling the direct copy of chemical information from a monolayer surface (the "master") to another surface of the same kind, so that, in principle, any replica could equally be used as master in the printing of new such replicas. Consequently, multiple parallel reproduction of a surface pattern, *via* the direct transfer of information from one generation of replicas to another, should become possible without the need to repeatedly reuse an expensive and difficult to produce master in the fabrication of each new replica. As demonstrated by the successful repeated reuse of the monolayer stamp pattern used in the agarose-mediated CER experiment described here (Figures 3, 10, and 11), this may be achievable with highly stable oranosilane monolayer patterns which, unlike, for example, alkanethiol monolayers on gold,[49,50] are not degraded even in rather harsh chemical and electrochemical environments.
- CER operates on the sole basis of wetting discrimination between the hydrophilic and hydrophobic regions of a monolayer stamp pattern, using flat, rigid monolayer stamps, and equally flat and rigid target surfaces consisting of a compact and extremely robust organosilane monolayer (OTS/Si) with an outer top surface that is both lyophobic (liquid repellent) and chemically inert. Such patterns can be printed on preassembled monolayer films covering the entire surface of the stamp or the target. These features render CER compatible with a wide range of postpatterning chemical modification processes[2,7,14] that are further expected to be free of lateral diffusion limitations of the kind encountered in μCP[1,17,20] and DPN[23,24] (which also led to the advancement of flat[20,21] and ink-free[18,19] versions of μCP).
- Because patterns are generated nondestructively on a stable, densely packed, and highly ordered monolayer rather than destructively (*e.g.*, nanoshaving[51]) or by deposition of material on a bare surface that needs to be backfilled with a second monolayer component which may partially displace the initially deposited material (e.g., μCP, DPN),[1,17,24] the CL−CER mode of patterning appears ideally suited for the assembly of monolayer template patterns with sharp, "seamless" boundaries between the different components of the pattern, as demanded by surface manipulation with true molecular resolution.
- Being an inherently parallel method of patterning, CER is capable of fast processing of information re-

gardless of the overall size of the pattern involved in the process. Extended down to the nanoscale, CER would provide a simple and straightforward means also for one-step replication of master nanopatterns serially created with a scanning probe or with an array of scanning probes;[25] with other words, CER would allow the unprecedented "upgrading" of a serial (slow) patterning process to a parallel (fast) one without losing the miniaturization advantage inherent in the serial process. Promising preliminary results in this direction, aiming at one-step electrochemical replication of tip-inscribed monolayer nanopatterns, have recently been obtained in this laboratory and will be reported in forthcoming publications.

EXPERIMENTAL SECTION

Water. Water purity, particularly with respect to organic contaminants, plays a critical role in the preparation of highly hydrophilic surfaces such as those needed for the assembly of high quality silane monolayers[15] or in the fabrication of contact electrochemical stamps (*vide infra*). All operations involving the use of pure water were carried out with water freshly withdrawn from a Barnstead Nanopure Diamond UV/UF system equipped with a total organic carbon (TOC) monitor and fed with water prepurified by reverse osmosis, ion exchange, and passage through 1 and 0.45 μm prefilters, which delivers ion-free and organic-free high purity water (18.2 MΩ cm, TOC less than 1 ppb).

Preparation of High Quality OTS/Si Monolayers. ***Cleaning of the Silicon Substrates.*** Silicon wafer substrates (Semiconductor Processing Co., Boston, double-side-polished, p-type, orientation <100>, resistivity 8−11 Ω cm, 0.5 mm thick, cut into ~20 mm × 40 mm or ~10 mm × 40 mm strips) covered by their native oxide layer were cleaned by the following sequence of operations: the silicon strips (mounted in a special quartz holder) are first rinsed in a jet of pure water (to remove dust and silicon particles from the surface), then Soxhlet extracted with toluene for 30 min (to remove soluble organic impurities), and then subjected to a version of the first step of the RCA cleaning procedure,[52] consisting of immersion for 10 min in a mixture of 50 mL of pure H_2O + 10 mL of NH_4OH (25%) + 10 mL of H_2O_2 (30%) in a quartz container thermostatted in a water bath at 68 °C. The RCA solution is quenched by overflowing it with pure water while the silicon strips remain submerged in liquid until the ambient temperature is reached, then the wet silicon strips are rapidly transferred to a beaker filled with pure water, rinsed under overflow for 10 min, and finally stored under pure water until use. To prevent contamination, the wafers must be cleaned shortly before the assembly of the monolayer. Silicon freshly cleaned by this procedure is perfectly hydrophilic (0° advancing and receding water contact angle) and so well suited for the assembly of high quality silane monolayers.[15]

Monolayer Self-Assembly. OTS/Si monolayers were assembled following a recently improved two-step procedure: (i) Freshly cleaned Si substrates, withdrawn from pure water and blown dry with clean, dry nitrogen withdrawn from a container of liquid nitrogen, are immersed for *ca.* 30 s in a 5 mM solution of OTS (Merck "For Synthesis" grade) in bicyclohexyl (BCH, Fluka, purified by percolation through basic alumina[53]) at 21−22 °C, followed by sonication for *ca.* 2 min in analytical-grade toluene (Frutarom). The immersion in the OTS/BCH adsorption solution and the toluene rinse are repeated once again. (Important: BCH was found to be ideally suited for use as solvent in the assembly of high-quality silane monolayers.[15]) OTS-covered surfaces prepared by this procedure emerge totally unwetted from the adsorption solution; (ii) elimination of monolayer defects by further densification and stabilization,[7] by exposure of the OTS-coated specimens for 12 h to a water saturated atmosphere (100% RH at 40 °C), followed by additional immersion in the OTS/BCH solution for *ca.* 30 s, sonication in toluene, and final annealing for 10 min in a preheated oven at 115 °C. This sequence of operations is repeated three times, ending with the thermal annealing at 115 °C.[7] All monolayer assembly operations were carried out at 50%−60% RH and 22 ± 1 °C, in a humidity-temperature controlled vertical laminar flow hood (total-exhaust, Germfree Biofume, Class II). (Important: performing the monolayer assembly operations within this range of ambient humidity appears to optimize the thickness of the hydration layer present on hydrophilic silicon surfaces, which is a key parameter for successful assembly of high quality silane monolayers.[15])

As determined by quantitative infrared measurements, densified OTS/Si monolayers assembled according to this experimental protocol contain 3%−6% more OTS material then those produced without densification (see Supporting Information, Figures S3 and S4) and display hysteresis-free static contact angles (equal advancing and receding values) of 116°−117° with water, 57° with bicyclohexyl, and 53° with *n*-hexadecane. These contact angle values are slightly but consistently higher (by 1°−2°) then those measured on same OTS/Si monolayers prior to their densification and stabilization.

Fabrication of the Monolayer Stamp Micropatterns. ***Photocleavage Patterning Step (Figure 2A,B).*** TEM grids mounted in a Teflon holder were cleaned by Soxhlet extraction with toluene, followed by exposure for ~30 s to HNO_3 vapor, then thoroughly rinsed in pure water (overflow) and finally dried in a stream of clean nitrogen. A specially built stainless steel irradiation holder was used to immobilize and firmly press a freshly cleaned grid with its smooth side against an OTS/Si specimen, the grid being covered with a thin quartz window. UV irradiation (2 h, λ = 185 nm) of the grid/OTS/Si assembly (through a small aperture in the stainless steel holder) was performed in a UV cleaner equipped with Hg-vapor lamps (model NL-UV 253, NLE, Nagoya, Japan), under argon purge (Ar purity, 99.9999%), in order to maintain a clean environment and avoid formation of ozone and undesired growth of silicon oxide.[6] Irradiated specimens were stored overnight in 10% aqueous HCl, then thoroughly rinsed in pure water and finally cleaned by the same RCA procedure as the pristine silicon substrates (*vide supra*). Patterned monolayer specimens were stored under pure water until further use.

NTS Assembly and Conversion to NTSox (Figure 2C,D; Figure 12). The assembly of an NTS/Si monolayer in the irradiated areas of photopatterned specimens (Figure 2) was done in exactly the same manner as the first step in the procedure applied to the assembly of the OTS/Si monolayers (*vide supra*). Specimens were withdrawn from water and blown dry with clean nitrogen immediately before their immersion in the NTS/BCH solution. NTS (10% stock solution in chloroform) was obtained from Prof. K. Ogawa, Kagawa University, Takamatsu, Japan

In the case of bilayer assembly (Figure 12), specimens used after their optical and IR or SFM characterization were reconditioned by immersion for 2 h in 10% aqueous HCl, followed by thorough rinsing with pure water (overflow). No reconditioning was needed when the assembly of the top NTS monolayer followed immediately after the printing of the bottom OTSeo@OTS monolayer pattern.

The conversion of NTS to NTSox, *via* oxidation with the $KMnO_4$/crown ether (dicyclohexano-18-crown-6) complex in benzene[4,35,53] was done by immersion (for 12 h) in a 5 mM solution of the crown ether complex (Sigma, mixed isomers) in analytical grade bezene (Fluka) under dry nitrogen, followed by sonication (5−10 min) in clean benzene, immersion in 10% aqueous HCl for *ca.* 5 h, and then a final thorough rinse in pure water (overflow). Specimens were stored under water and used shortly after the conversion of NTS to NTSox.

Glycerol/Monolayer Micropatterns. The assembly of glycerol (J. T. Baker, anhydrous) on monolayer patterns was performed as depicted in Figure 6, by slowly pulling out (with the help of a motor-driven lift) the specimen bearing the monolayer micropat-

tern from the neat liquid at the ambient temperature (22 ± 0.5 °C).

Agarose/Monolayer Micropatterns. Water solutions of agarose (adjusted to a final concentration of 0.1 wt %) were prepared by dissolving agarose powder (Sigma, type VII-A, low gelling temperature, melting temp ≤ 65.5 °C) with stirring in pure water at the ambient temperature and then heating up to 95 °C for 5 min. The solutions were passed twice (at 60 °C) through a Millipore membrane filter (Durapore 0.1 μm) and then extracted at least four times with 2-pentanol (at ~50 °C), to remove impurities (apparently surfactant compounds) that promote undesired surface contamination of the OTS/Si monolayers with material from solution. The bulk gelation of 0.1 wt % agarose solutions prepared by this procedure was found to occur at 16−21 °C, and is expected to shift toward higher temperatures as the concentration of surface-immobilized agarose features increases[54] upon loss of water by evaporation.

The assembly of agarose on monolayer patterns was done from such freshly prepared agarose solutions at 90 °C, in the same manner as that of glycerol (*vide supra*).

The removal of agarose gel features assembled on NTXox or OTSeo monolayers, or transferred to the OTSeo replica features generated in the CER process with agarose stamps, was done by soaking for 2 min in pure boiling water and then in 10% aqueous HCl for 2 h at the ambient temperature, in order to remove a residual ultrathin layer of agarose that is not soluble in water. Preliminary IR data suggest that this water-insoluble residue may be a single monolayer of agarose bound covalently to the silane monolayer *via* ester bonds formed between the −OH groups of the agarose and the −COOH functions of NTXox or OTSeo.

Water Condensation Patterns. Control of the water condensation on the monolayer patterns was achieved in a specially built perspex cell equipped with a humidity sensor and a Peltier element that can be used to slowly vary the surface temperature of the specimen bearing the monolayer pattern and stabilize it within ± 0.1 °C. The relative humidity in the cell can be controlled within ~5% using a pair of small beakers filled with water or with various constant humidity salt solutions. A porous cellulose wick dipped into the liquid is used to increase the effective area of the liquid−vapor interface and so speed up the attainment of the equilibrium relative humidity. Continuous optical monitoring of the formation and disappearance of water patterns is realized (through a transparent glass window in the center of the perspex cover of the cell) with the help of a zoom lens system (Navitar) equipped with a digital camera connected to a computer.

Contact Electrochemical Replication Experiments. The CER experiments were carried out in a cell similar to that used for the control of the water condensation, equipped, in addition to the humidity sensor and the Peltier element, with stainless steel holders for the stamp and the target specimens that are electrically connected to a stabilized dc voltage generator, the output of which may be continuously varied in the range 3−80 V. We are experimenting with different types of electrical contacts to the stamp and the target. In the experiments reported here, pieces of flexible aluminum foil glued with adhesive tape were used to improve the holder-stamp and holder-target electrical contact; however, the effectiveness and reproducibility of electrical contacts is an important technical issue that remains to be addressed in future work. The upper holder (stamp) is mobile and may be pressed against the bottom holder (target) with variable mechanical force, manually or using calibrated weights. *In-situ* optical imaging of the stamp and target is not possible in this cell.

SFM Imaging. The wide scan SFM images (200 μm × 200 μm) needed in this study for the correlation of the SFM with the micro-FTIR data were acquired on an NTEGRA instrument (NT-MDT, Moscow, Russia) operated in the DualScan mode, which provides the option of simultaneous scanning by both sample and probe. In hydrogel experiments demanding deliberate variation of the ambient humidity, the sample compartment (equipped with a humidity sensor) was purged with dry or humidified nitrogen supplied from a RH-controlled humidifier specially built for this purpose.

Infrared Spectral Measurements. Quantitative FTIR spectra in the Brewster angle configuration[35] (Figure 5) were acquired (at a resolution of 4 cm^{-1}) as described before,[35,53,15] on a Nicolet 730 FTIR system equipped with a DTGS detector, wire grid ZnSe polarizer, and a computer controlled "shuttle" accessory that allows automatic translation of the sample in and out of the IR beam during data acquisition. Quantitative micro-FTIR transmission spectra (Figures 8, 9, 11, 12) were acquired (at a resolution of 4 cm^{-1}) on a Bruker Equinox 55 spectrometer connected to an IRscope II infrared microscope accessory equipped with a liquid nitrogen-cooled MCT detector. The infrared microscope is also used as an optical microscope (equipped with a computer-connected digital camera) for optical imaging and selection of sample regions from which IR spectra are to be recorded (see Figure 11). (Important: The use of double-side-polished silicon coated on the back side with a lyophobic monolayer like OTS or NTS is necessary to protect the samples from adventitious contamination that may add undefined spectral features to the measured infrared spectra.)

All displayed spectral curves represent net spectral contributions of the respective surface coatings, after mathematical subtraction of the spectral contributions of the corresponding bare silicon substrates.

Acknowledgment. This research was supported by the Israel Science Foundation (Grant No. 1109/04). The NTS material was kindly supplied by Prof. Kazufumi Ogawa of Kagawa University, Takamatsu, Japan.

Supporting Information Available: Humidity effects on agarose micropatterns; FTIR spectra demonstrating addition of monolayer material upon densification. This material is available free of charge *via* the Internet at http://pubs.acs.org.

REFERENCES AND NOTES

1. See, for example: Gates, B. D.; Xu, Q.; Stewart, M.; Ryan, D.; Willson, C. G.; Whitesides, G. M. New Approaches to Nanofabrication: Molding, Printing, and Other Techniques. *Chem. Rev.* **2005**, *105*, 1171–1196.
2. Maoz, R.; Frydman, E.; Cohen, S. R.; Sagiv, J. Constructive Nanolithography: Inert Monolayers as Patternable Templates for In-situ Nanofabrication of Metal-Semiconductor-Organic Surface Structures—A Generic Approach. *Adv. Mater.* **2000**, *12*, 725–731.
3. Hoeppener, S.; Maoz, R.; Sagiv, J. Constructive Microlithography: Electrochemical Printing of Monolayer Template Patterns Extends Constructive Nanolithography to the Micrometer—Millimeter Dimension Range. *Nano Lett.* **2003**, *3*, 761–767.
4. Maoz, R.; Cohen, S. R.; Sagiv, J. Nanoelectrochemical Patterning of Monolayer Surfaces: Toward Spatially Defined Self-Assembly of Nanostructures. *Adv. Mater.* **1999**, *11*, 55–61.
5. Maoz, R.; Frydman, E.; Cohen, S. R.; Sagiv, J. Constructive Nanolithography: Site-Defined Silver Self-Assembly on Nanoelectrochemically Patterned Monolayer Templates. *Adv. Mater.* **2000**, *12*, 424–429.
6. Hoeppener, S.; Maoz, R.; Cohen, S. R.; Chi, L.; Fuchs, H.; Sagiv, J. Metal Nanoparticles, Nanowires, and Contact Electrodes Self-Assembled on Patterned Monolayer Templates—A Bottom-up Chemical Approach. *Adv. Mater.* **2002**, *14*, 1036–1041.
7. Liu, S.; Maoz, R.; Sagiv, J. Planned Nanostructures of Colloidal Gold *via* Self-Assembly on Hierarchically Assembled Organic Bilayer Template Patterns with *in-situ* Generated Terminal Amino Functionality. *Nano Lett.* **2004**, *4*, 845–851.
8. Onclin, S.; Ravoo, B. J.; Reinhoudt, D. N. Engineering Silicon Oxide Surfaces Using Self-Assembled Monolayers. *Angew. Chem., Int. Ed.* **2005**, *44*, 6282–6304.
9. Cai, Y.; Ocko, B. M. Electro Pen Nanolithography. *J. Am. Chem. Soc.* **2005**, *127*, 16287–16291.
10. Checco, A.; Cai, Y. G.; Gang, O.; Ocko, B. M. High Resolution Non-Contact AFM Imaging of Liquids Condensed onto

Chemically Nanopatterned Surfaces. *Ultramicroscopy* **2006**, *106*, 703–708.
11. Hoeppener, S.; Susha, A. S.; Rogach, A. L.; Feldmann, J.; Schubert, U. S. Guided Self-Assembly of Fe_3O_4 Nanoparticles on Chemically Active Surface Templates Generated by Electro-Oxidative Nanolithography. *Curr. Nanosci.* **2006**, *2*, 135–141.
12. Becer, C. R.; Haensch, C.; Hoeppener, S.; Schubert, U. S. Patterned Polymer Brushes Grafted from Bromine-Functionalized, Chemically Active Surface Templates. *Small* **2007**, *3*, 220–225.
13. Andruzzi, L.; Nickel, B.; Schwake, G.; Rädler, J. O.; Sohn, K. E.; Mates, T. E.; Kramer, E. J. Bio-Selective Surfaces by Chemically Amplified Constructive Microlithography. *Surf. Sci.* **2007**, *601*, 4984–4992.
14. Chowdhury, D.; Maoz, R.; Sagiv, J. Wetting Driven Self-Assembly as a New Approach to Template-Guided Fabrication of Metal Nanopatterns. *Nano Lett.* **2007**, *7*, 1770–1778.
15. Wen, K.; Maoz, R.; Cohen, H.; Sagiv, J.; Gibaud, A.; Desert, A.; Ocko, B. M. Postassembly Chemical Modification of a Highly Ordered Organosilane Multilayer: New Insights into the Structure, Bonding, and Dynamics of Self-Assembling Silane Monolayers. *ACS Nano* **2008**, *2*, 579–599.
16. Wouters, D.; Willems, R.; Hoeppener, S.; Flipse, C. F. J.; Schubert, U. S. Oxidation Conditions for Octadecyl Trichlorosilane Monolayers on Silicon: A Detailed Atomic Force Microscopy Study of the Effects of Pulse Height and Duration on the Oxidation of the Monolayer and the Underlying Si Substrate. *Adv. Funct. Mater.* **2005**, *15*, 938–944.
17. Smith, R. K.; Lewis, P. A.; Weiss, P. S. Patterning Self-Assembled Monolayers. *Prog. Surf. Sci.* **2004**, *75*, 1–68.
18. Loo, Y.-L.; Willett, R. L.; Baldwin, K. W.; Rogers, J. A. Interfacial Chemistries for Nanoscale Transfer Printing. *J. Am. Chem. Soc.* **2002**, *124*, 7654–7655.
19. Li, X.-M.; Péter, M.; Huskens, J.; Reinhoudt, D. N. Catalytic Microcontact Printing Without Ink. *Nano Lett.* **2003**, *3*, 1449–1453.
20. Sharpe, R. B. A.; Burdinski, D.; Huskens, J.; Zandvliet, H. J. W.; Reinhoudt, D. N.; Poelsema, B. Chemically Patterned Flat Stamps for Microcontact Printing. *J. Am. Chem. Soc.* **2005**, *127*, 10344–10349.
21. Coyer, S. R.; García, A. J.; Delamarche, E. Facile Preparation of Complex Protein Architectures with Sub-100-nm Resolution on Surfaces. *Angew. Chem.* **2007**, *119*, 6961–6964.
22. Piner, R. D.; Zhu, J.; Xu, F.; Hong, S. H.; Mirkin, C. A. "Dip-Pen" Nanolithography. *Science* **1999**, *283*, 661–663.
23. Zhang, H.; Chung, S. W.; Mirkin, C. A. Fabrication of Sub-50-nm Solid-State Nanostructures on the Basis of Dip-Pen Nanolithography. *Nano Lett.* **2003**, *3*, 43–45.
24. Krämer, S.; Fuierer, R. R.; Gorman, C. B. Scanning Probe Lithography Using Self-Assembled Monolayers. *Chem. Rev.* **2003**, *103*, 4367–4418.
25. Mirkin, C. A. The Power of the Pen: Development of Massively Parallel Dip-Pen Nanolithography. *ACS Nano* **2007**, *2*, 79–83.
26. Sun, S.; Montague, M.; Critcheley, K.; Chen, M.-S.; Dressick, W. J.; Evans, S. D.; Leggett, G. J. Fabrication of Biological Nanostructures by Scanning Near-Field Photolithography of Chloromethylphenylsiloxane Monolayers. *Nano Lett.* **2006**, *6*, 29–33.
27. Garcia, R.; Martinez, R. V.; Martinez, J. Nano-Chemistry and Scanning Probe Nanolithographies. *Chem. Soc. Rev.* **2006**, *35*, 29–38.
28. García, R.; Calleja, M.; Rohrer, H. Patterning of Silicon Surfaces with Noncontact Atomic Force Microscopy: Field-Induced Formation of Nanometer-Size Water Bridges. *J. Appl. Phys.* **1999**, *86*, 1898–1903.
29. Cavallini, M.; Mei, P.; Biscarini, F.; García, R. Parallel Writing by Local Oxidation Nanolithography with Submicrometer Resolution. *Appl. Phys. Lett.* **2003**, *83*, 5286–5288.
30. Yokoo, A. Nanoelectrode Lithography and Multiple Patterning. *J. Vac. Sci. Technol., B* **2003**, *21*, 2966–2969.
31. Hoeppener, S.; Maoz, R.; Sagiv, J. Contact Electrochemical Replication of Electrochemically Printed Monolayer Patterns. *Adv. Mater.* **2006**, *18*, 1286–1290.
32. Möhwald, H.; Höhne, U.; Quint, P. Dynamics of Structure Formation in Model Membranes and in Adsorbed Layers. *Polym. J.* **1991**, *23*, 583–592.
33. Calvert, J. M.; Georger, J. H.; Peckerar, M. C.; Pehrsson, P. E.; Schnur, J. M.; Schoen, P. E. Deep UV Photochemistry and Patterning of Self-Assembled Monolayer Films. *Thin Solid Films* **1992**, *210/211*, 359–363.
34. Gau, H.; Herminghaus, S.; Lenz, P.; Lipowsky, R. Liquid Morphologies on Structured Surfaces: From Microchannels to Microchips. *Science* **1999**, *283*, 46–49.
35. Maoz, R.; Sagiv, J.; Degenhardt, D.; Möhwald, H.; Quint, P. Hydrogen-Bonded Multilayers of Self-Assembling Silanes: Structure Elucidation by Combined Fourier Transform Infrared Spectroscopy and X-ray Scattering Techniques. *Supramol. Sci.* **1995**, *2*, 9–24.
36. Local degradation of OTS monolayers, accompanied by growth of silicon oxide, was observed in lithography with scanning SFM tips at applied bias voltages exceeding certain threshold values, which depend on ambient relative humidity,[2] pulse duration,[16] and the performance of each particular tip.[2,16,7,14]
37. Nuzzo, R. G.; Dubois, L. H.; Allara, D. L. Fundamental Studies of Microscopic Wetting on Organic Surfaces. 1. Formation and Structural Characterization of a Self-Consistent Series of Polyfunctional Organic Monolayers. *J. Am. Chem. Soc.* **1990**, *112*, 558–569.
38. Fontaine, P.; Goguenheim, D.; Deresmes, D.; Vuillaume, D. Octadecyltrichlorosilane Monolayers as Ultrathin Gate Insulating Films in Metal-Insulator-Semiconductor Devices. *Appl. Phys. Lett.* **1993**, *62*, 2256–2258.
39. This current density is lower than the values usually obtained in studies of electron transport through *n*-alkane thiols sandwiched between two metal electrodes,[40] and comparable to the maximal values reported for C18 Si-bound *n*-alkyl monolayers contacted through a liquid Hg drop,[41] the latter being, however, recorded with applied bias voltages below 1 V.
40. Salomon, A.; Cahen, D.; Lindsay, S.; Tomfohr, J.; Engelkes, V. B.; Frisbie, C. D. Comparison of Electronic Transport Measurements on Organic Molecules. *Adv. Mater.* **2003**, *15*, 1881–1890.
41. Salomon, A.; Boecking, T.; Chan, C. K.; Amy, F.; Girshevitz, O.; Cahen, D.; Kahn, A. How Do Electronic Carriers Cross Si-Bound Alkyl Monolayers? *Phys. Rev. Lett.* **2005**, *95*, 266807-1–266807-4.
42. Itagaki, H.; Fukiishi, H.; Imai, T.; Watase, M. Molecular Structure of Agarose Chains in Thermoreversible Hydrogels Revealed by Means of a Fluorescent Probe Technique. *J. Polym. Sci., B* **2005**, *43*, 680–688.
43. Venyaminov, S. Y.; Prendergast, F. G. Water (H_2O and D_2O) Molar Absorptivity in the 1000−4000 cm^{-1} Range and Quantitative Infrared Spectroscopy of Aqueous Solutions. *Anal. Biochem.* **1997**, *248*, 234–245.
44. Bellamy, L. J. *The Infrared Spectra of Complex Molecules*, 3rd ed.; Chapman & Hall: London, 1975.
45. *Aldrich Library of FT-IR Spectra*, 2nd ed.; Aldrich: Milwaukee, WI, 1997.
46. Darhuber, A. A.; Troian, S. M.; Davis, J. M.; Miller, S. M.; Wagner, S. Selective Dip-Coating of Chemically Micropatterned Surfaces. *J. Appl. Phys.* **2000**, *88*, 5119–5126.
47. Good IR measurements of the water content of the gel at ambient humidity higher than ~60% RH could not be performed because of the interference with the strong infrared bands of water in the gas phase.
48. Kaholek, M.; Lee, W.-K.; LaMattina, B.; Caster, K. C.; Zauscher, S. Fabrication of Stimulus-Responsive Nanopatterned Polymer Brushes by Scanning-Probe Lithography. *Nano Lett.* **2004**, *4*, 373–376.

49. Schoer, J. K.; Zamborini, F. P.; Crooks, R. M. Scanning Probe Lithography. 3. Nanometer-Scale Electrochemical Patterning of Au and Organic Resists in the Absence of Intentionally Added Solvents or Electrolytes. *J. Phys. Chem.* **1996**, *100*, 11086–11091.
50. Jang, J.-W.; Sanedrin, R. G.; Maspoch, D.; Hwang, S.; Fujigaya, T.; Jeon, Y.-M.; Vega, R. A.; Chen, X.; Mirkin, C. A. Electrically Biased Nanolithography with KOH-Coated AFM Tips. *Nano Lett.* **2008**, *8*, 1451–1455.
51. Liu, G.-Y.; Xu, S.; Qian, Y. Nanofabrication of Self-Assembled Monolayers Using Scanning Probe Lithography. *Acc. Chem. Res.* **2000**, *33*, 457–466.
52. Kern, W.; Puotinen, D. A. Cleaning Solutions Based on Hydrogen Peroxide for Use in Silicon Semiconductor Technology. *RCA Rev.* **1970**, *31*, 187–206.
53. Frydman, E.; Cohen, H.; Maoz, R; Sagiv, J. Monolayer Damage in XPS Measurements as Evaluated by Independent Methods. *Langmuir* **1997**, *13*, 5089–5106.
54. Mohammed, Z. H.; Hember, M. W. N.; Richardson, R. K.; Morris, E. R. Kinetic and Equilibrium Processes in the Formation and Melting of Agarose Gels. *Carbohydr. Polym.* **1998**, *36*, 15–26.